https://doi.org/10.5194/egusphere-2023-968
Preprint. Discussion started: 22 May 2023

Disentangling the effect of geomorphological features and tall shrubs on snow depth variation in a sub-Arctic watershed using UAV derived products

Ian Shirley[1], Sebastian Uhlemann[1], John Peterson[1], Katrina Bennett[2], Susan S. Hubbard[3], Baptiste Dafflon[1]

[1]Lawrence Berkeley National Laboratory, Berkeley, CA, USA
[2]Los Alamos National Laboratory, Los Alamos, NM, USA
[3]Oak Ridge National Laboratory, Oak Ridge, TN, USA

Correspondence to: Ian Shirley (IShirley@lbl.gov)

Abstract. Spatial variation in snow depth is a main driver of heterogeneity in discontinuous permafrost landscapes, exerting a strong control on thermal and hydrological processes, vegetation dynamics, and carbon cycling. Topography and vegetation are understood to play an important role in driving variation in snow depth, but complex morphology often impedes efforts to disentangle these drivers. Maps of ground, vegetation and snow surface elevation were collected using an Unmanned Aerial Vehicle (UAV) over multiple years across a watershed on the Seward Peninsula in Alaska. Here, we quantify drivers of snow depth variation using the inferred maps of snow depth during peak snow accumulation in 2019 and 2022 and collocated ground surface elevation and vegetation height. A novel approach to extract microtopographic information from complex landscape morphologies is used to classify different features (e.g. drainage paths, risers and terraces, thermokarst patterned ground) and characterize their relationships with snow depth variation. A simple model developed using topographic information alone is shown to correlate strongly with local snow depth variation where vegetation height is low. We build a machine learning model to quantify snow trapping by shrub canopies in the watershed and show that snow trapping can be characterized by an exponential function of canopy height above snow (RMSE = 0.12 m, R^2 = 0.5). Finally, we demonstrate that relationships between microtopography, vegetation height, and snow depth hold in years of deep and shallow snowpack. These results can be applied to improve representation of heterogeneity and vegetation-snow feedbacks in Earth System Models and to increase the spatial resolution of pan-arctic estimates of snow depth.

1 Introduction

Snow is a key component of high-latitude ecosystem dynamics. Snow warms high-latitude soils by insulating the ground surface from frigid winter air temperature, but the level of insulation provided varies strongly with snow depth (Zhang, 2005). In discontinuous permafrost environments, where mean annual air temperatures approach 0 C, snow depth controls the ability of permafrost to develop and persist (Smith and Riseborough, 2002). In these environments, local variation in

https://doi.org/10.5194/egusphere-2023-968
Preprint. Discussion started: 22 May 2023

snow depth can lead to coexistence of permafrost and talik (perennially unfrozen) soils in close proximity (Uhlemann et al., 2021; Zoltai, 1993). Via its impact on soil thermal regimes, spatial variation in snow depth is a primary driver of landscape heterogeneity in discontinuous permafrost environments, exerting a strong control on hydrological processes, vegetation dynamics, and carbon cycling (Shirley et al., 2022). Because of this, understanding of high-latitude biosphere-atmosphere interactions would benefit from improved characterization and prediction of snow depth variation, particularly in discontinuous permafrost environments.

In high-arctic polygonal tundra, ice-wedges create repeatable and recognizable microtopographic features over largely flat landscapes. In these relatively simple morphological landscapes, researchers have been able to identify strong associations between snow depth and microtopographic position using digital elevation maps (Wainwright et al., 2017). Most high-latitude environments, however, are more topographically complex and delineation of microtopographic features is more challenging. Microtopography created by thermokarst thaw slumps, solifluction lobes, hillslope terraces, and drainage paths is irregular, and is typically masked in digital elevation models by sloping or mountainous terrain. In these environments, associations between microtopography and snow depth have been suggested using fractal dimensionality (Deems et al., 2006) and topographic indices like curvature (Dvornikov et al., 2015; Revuelto et al., 2020), but these associations have not been developed for snow depth prediction. Recent work has leveraged topographic information to predict snow depth variation using machine learning algorithms (Bennett et al., 2022; Meloche et al., 2022), but interpretation of machine learning models is challenging and their scope may be limited to the spatial domain in which they were trained (Shirley et al., 2023). More effort is needed, therefore, to identify explicit relationships between terrain morphology and snow depth variation that can be used to advance understanding and prediction of snow depth across the high-latitudes.

At high–latitudes, an association between shrubs and deeper than average snow depths has been well established (Frost et al., 2018; Myers-Smith and Hik, 2013; Sturm et al., 2005). This association has largely been attributed to snow trapping by shrub canopies, and such physical trapping effects have been demonstrated using snow fences and other experimental manipulations (Myers-Smith and Hik, 2013; Wipf and Rixen, 2010; O'Neill and Burn, 2017). However, in these cold

https://doi.org/10.5194/egusphere-2023-968
Preprint. Discussion started: 22 May 2023

environments, shrubs benefit from deeper snowpacks due to increased nitrogen mineralization and uptake (Sturm et al., 2005; Shirley et al., 2022), so it is also possible that they preferentially grow in landscape positions covered by deeper snowpacks. In complex topographical shrublands, therefore, separating the influence of canopy trapping and topographic position on snow depth presents a challenge.

In this work, we develop tools to separate and quantify drivers of snow depth variation at the landscape scale to test the hypothesis that local variation in snow depth is driven by both topography and vegetation in these landscapes. Using an Unmanned Aerial Vehicle (UAV), we inferred maps of ground elevation, vegetation height, and snow depth during peak snow accumulation in 2019 and 2022, across a watershed on the Seward Peninsula in Alaska. Here, we develop a novel approach to extract microtopographic features from complex landscape morphologies and use it to characterize relationships between microtopography and snow depth across the watershed. In particular, we show that patterns of snow accumulation differ between topographic features (e.g. drainage paths, risers and terraces, thermokarst patterned ground). Then we leverage the above topographic analysis in conjunction with machine learning algorithms to quantify shrub canopy snow trapping in the watershed, and examine how this trapping varies with terrain, wind direction, and shrub distribution. Finally, we compare the interactions between microtopography, vegetation height, and snow depth in 2019, when the watershed was covered by a deep snowpack, and in 2022, when the watershed was covered by a much shallower snowpack.

2 Data and Methods

2.1 Study Site

This study is focused on a watershed located about 40 km northwest of Nome on the Seward Peninsula in Alaska (64.72°N, 165.94°W). This watershed (Teller 27) has been the subject of extensive investigation by the Next-Generation Ecosystem Experiment (NGEE) Arctic project (Uhlemann et al., 2021; Bennett et al., 2022; Léger et al., 2019; Shirley et al., 2022). The watershed, which covers an area of approximately 2.3 km^2, is characterized by a 130 m elevation gradient and is underlain by discontinuous permafrost (Uhlemann et al., 2021). Three main types of topographic features are present in the study domain. A stream that cuts through the center of the watershed is the most prominent topographic feature. The midslope

https://doi.org/10.5194/egusphere-2023-968
Preprint. Discussion started: 22 May 2023

region is characterized by a series of risers and terraces that cut perpendicular to the primary slope direction. The flatter regions at the top and bottom of the watershed are characterized by thermokarst patterned ground, with raised patches of near-surface permafrost distributed among lower wetland areas with deeper active layers. The watershed is covered by low-lying tundra vegetation (dwarf shrubs, bryophytes, graminoids, and sedges) interspersed with patches of deciduous willow shrubs (Salix spp) ranging in height from 0.5 to 3 m (Konduri et al., 2022).

2.2 Maps of snow depth, surface elevation, and vegetation height collected using UAV

In order to produce maps of snow depth, topography, and vegetation height, UAV photogrammetric surveys were conducted across the watershed. This technique has been established as an effective way to map snow depth in high-latitude and mountainous terrain (Wainwright et al., 2017; Fernandes et al., 2018; Nolan et al., 2015; Goetz and Brenning, 2019). A number of studies have performed extensive evaluation of photogrammetric methods for snow depth mapping and have demonstrated the effectiveness of this cost-effective and efficient method (Revuelto et al., 2021; Harder et al., 2020, 2016; Avanzi et al., 2018; Goetz and Brenning, 2019). The RMSE of photogrammetric snow depth measurements in these studies ranges from less than 10 cm to 30 cm across a variety of terrain types and snow conditions.

In this study, multiple photogrammetric surveys involving a UAV-mounted digital camera (Matrice 210 with X5S camera, DJI) and Ground Control Points (GCPs) were performed to map the surface elevation at various times of year and infer vegetation height and snow depth spatial variability across the studied watershed. The surveys covered ~1.7 km^2 of the 2.2 km^2 watershed with missing areas located along the edges of the watershed. Each survey consisted of 7-10 UAV flights at an elevation between 70 and 100 m above ground surface, providing imagery with a ground resolution in the order of 2 to 5 cm. The GCPs involved approximately 50 targets that were surveyed with a Real Time Kinematic (RTK)-GPS. The GCPs were used in conjunction with the UAV-based imagery to generate surface elevation models with 10 cm grid cell size using a structure-from-motion-based reconstruction software (Agisoft Metashape) (Dafflon et al., 2016; James and Robson, 2012; Wainwright et al., 2017). Surface elevation models were inferred for multiple dates representing times of year close to

https://doi.org/10.5194/egusphere-2023-968
Preprint. Discussion started: 22 May 2023

highest plant and leaf density (July 19, 2017), maximum snow depth (April 1, 2019, and April 11, 2022), and low plant and leaf density after the first bare-ground date (June 9, 2019).

Several products were created from the surface elevation models. We generated a digital terrain model (DTM) proxy from the June 9 2019 surface elevation model by keeping and interpolating only the grid cells with values that were less than 0.5 m higher than the minimum value in a centered 5 m side window. This approach aimed at removing grid cells that were linked to the presence of willow branches and/or early leaves, with the caveat of slightly smoothing the elevation change at geomorphological features boundaries. Vegetation height and snow depth products were obtained by subtracting the DTM from the snow and vegetation surface elevation models (April and July datasets respectively). The comparison of the generated products with RTK-GPS measurement along several transects indicate a RMSE of 16 cm for the snow depth product and an RMSE of 17 cm for the terrain proxy (Figure 2). Some of this error may be attributed to the accuracy of the RTK-GPS and snow probe measurements. We consider the overall quality of the dataset to be high, with the largest errors present along the edge of terraces, which are smoothed in the terrain proxy, and a few locations in dense willow patches.

2.3 Stacked directional filtering

Fine-scale topographic features present in the studied watershed, even if they are easily identified on the ground (such as hummocks) are masked in the watershed DTM by coarser-scale topographic variation (Figs. 1,4). Standard metrics to extract topographic information like topographic position index operate at a single spatial scale, result in strong smoothing of the underlying terrain, and are blind to directional dependence of topographic variations. Therefore, these metrics are not well suited for use in highly heterogeneous landscapes (Reu et al., 2013). Here, we develop a filtering technique (stacked directional filtering) to extract topographic features from complex landscapes that preserves the spatial structure and sharpness of the features.

https://doi.org/10.5194/egusphere-2023-968
Preprint. Discussion started: 22 May 2023

In the stacked directional filtering approach, an image is iteratively filtered along perpendicular directions at increasingly coarse scales. At a given spatial scale i, the mean value along two perpendicular lines of length i ($\underline{z}_{i,m-i:m+i,n}$ and $\underline{z}_{i,m,n-i:n+i}$) is subtracted from the value of the central point ($z_{i,m,n}$) at every location m,n in the image (Eqs. (1),(2)). This creates two maps that contain the information content of the image at scale i and in each direction. These maps are subtracted from the base image to create a new base image for analysis at the next coarsest spatial scale (Eq. (3)). The process begins at the finest spatial scale and is iterated until the coarsest spatial scale of interest is reached. These maps can be analyzed individually for information at particular scales and directionalities, or summed to produce maps that have coarse features removed (Eq. (4)).

$$y_{1,i,m,n} = z_{i,m,n} - \underline{z}_{i,m-i:m+i,n}\,, \tag{1}$$

$$y_{2,i,m,n} = z_{i,m,n} - \underline{z}_{i,m,n-i:n+i}\,, \tag{2}$$

$$z_{i+1,m,n} = z_{i,m,n} - (y_{1,i,m,n} + y_{2,i,m,n}) \tag{3}$$

$$x_{i,m,n} = \sum_{j=i_0}^{i} (y_{1,j,m,n} + y_{2,j,m,n}) \tag{4}$$

In this work, we filter the DTM at scales that increase by 10 m from 11 m to 221 m. Directions 1 and 2 are chosen to be roughly parallel and perpendicular to the dominant hillslope direction (down-slope and cross-slope), respectively.

2.4 Extraction of topographic features

We use topographic maps to locate thermokarst patterned ground, terrace/riser features, and the stream feature in the watershed. For simplicity, we take the top part of the watershed as representative of thermokarst patterned ground. Filtered topographic images at 21 m scale are used to roughly extract the other features. The standard deviation of a 100 m by 100 m region centered on each location in the watershed is calculated for both the down-slope and cross-slope directions. The stream feature is classified by taking all points with standard deviation greater than 0.1 m in the cross-slope direction at this scale. Terrace/riser features are classified by taking points that are not part of the stream feature and have standard deviation greater than 0.07 m in the down-slope direction. Terrace/riser features identified in the bottom right quadrant of the

https://doi.org/10.5194/egusphere-2023-968
Preprint. Discussion started: 22 May 2023

watershed are excluded because of their proximity to patches of tall shrubs. The classified regions for each feature are shown in Fig. S2.

2.5 Simple topographic model of snow depth variation (TM_SV)

We created a simple model of snow depth variation in the watershed by performing a weighted sum of the stacked directional filtered topographic maps, with the weights determined by fitting filtered 2019 snow maps ($SD_{1,i,m,n}$ and $SD_{2,i,m,n}$) at a given scale to filtered topography maps ($y_{1,i,m,n}$ and $y_{2,i,m,n}$) at that same scale. For each scale i, ranging from 11 to 212 m, fit coefficients w_i are determined by performed a linear fit of $(y_{1,i,m,n} + y_{2,i,m,n})$ to ($SD_{1,i,m,n}$ and $SD_{2,i,m,n}$) with the intercept set to zero (Fig. S3). Snow depth variation (TM_SV) at each location m,n is modeled as the sum of these weighted topographic maps (Eq. (5)).

$$TM\_SV_{m,n} = \sum_{j=i_0}^{i} [w_i \times (y_{1,j,m,n} + y_{2,j,m,n})] \quad (5)$$

2.6 Shrub canopy snow trapping field

Snow trapping by objects like snow fences and shrub canopies depends on the shape of the object and extends beyond its edges. This means that a simple map of vegetation height cannot capture the spatial structure of canopy-intercepted snow. To better characterize the relationship between canopy structure and snow trapping, we introduce the shrub canopy snow trapping field. The shrub canopy snow trapping fields (ϕ_1 and ϕ_2) are defined at each point m,n as the sum of neighboring vegetation height (h_i) weighted by the inverse of the distance (r) to the power 1 and 2 (Eqs. (6), (7)). For computational efficiency, only shrubs that lie within a 50 m by 50 m window of each point contribute to ϕ_1 and ϕ_2. Here, we also limit the shrub height such that the maximum value of h_i is 1.5 m and normalize the values of ϕ_1 and ϕ_2 such that they range from 0 to 1.

$$\phi_1 = \sum_i h_i r_i^{-1} \quad (6)$$

https://doi.org/10.5194/egusphere-2023-968
Preprint. Discussion started: 22 May 2023

$$\phi_2 = \sum_i h_i r_i^{-2} \quad (7)$$

2.7 Machine-learning estimation of snow trapping by shrub canopies

To estimate the trapping of snow due to shrub canopies, we create a machine learning model of snow depth across the watershed using the following predictor variables: filtered maps at each scale and directionality (Section 2.3), the simple topographic model (Section 2.5), slope and aspect calculated using maps of z_i at each scale, elevation, vegetation height, shrub canopy snow trapping fields (ϕ_1 and ϕ_2; Section 2.6), and the gradients of the shrub canopy snow trapping fields in the cross-slope and down-slope directions. We use the boosted regression tree (BRT) algorithm, which excels at capturing non-linear response curves and interactions between variables (Elith et al., 2008). The BRT model is implemented in R using the 'gbm' package (Greenwell et al., 2020) with a gaussian error distribution, bag fraction of 0.5, tree complexity of 3, a learning rate of 0.03, and a tree number optimized with 10-fold cross-validation. Model performance is strongly dependent on the amount of data used for training. The model is trained using 15000 randomly selected data points, or ~2% of the full dataset, as this model performs only marginally better than a model trained with 5000 points. The model was used to predict snow depth across the watershed twice: first with the measured shrub height and potential, and then with the shrub height and shrub potential set to zero everywhere. The difference between these two maps is taken to be the amount of snow accumulated by shrub canopies throughout the watershed.

3 Results and Discussion

3.1 Topographic variation and snow redistribution

Using the novel technique of stacked directional filtering, we extracted scale- and direction-dependent information from the watershed DTM and 2019 snow depth maps (Fig. S1). Taking the standard deviation of each layer of the image stacks as a metric of relative importance, we find that topography varies across all scales while variation in snow depth is attenuated at

https://doi.org/10.5194/egusphere-2023-968
Preprint. Discussion started: 22 May 2023

scales larger than ~100 m (Fig. 3). We grouped 100 m by 100 m patches by topographic feature (excluding patches of tall shrubs) and compared the scale-dependence of topography and snow variation among the feature types (Fig. 3).

The thermokarst patterned ground at the top of the watershed is relatively flat at coarse scales, and the features are not characterized by strong directionality. Therefore, topographic variation is similar in both the down-slope and cross-slope directions, and peaks at the finest scales. For this type of terrain, snow variation is characterized by almost identical spatial trends as the topography.

The stream feature, in contrast, cuts across steeper terrain in the down-slope direction. Topographic variability is highest in the cross slope direction, peaking at scales of 40 m to 60 m. Cross-slope snow variation is also much higher in the stream feature than the rest of the watershed at all scales, although snow variability peaks at finer scales (20 m to 30 m) than topographic variability.

Terraces and risers run perpendicular to the hillslope direction. These features are characterized by more topographic variation in the downslope direction than the rest of the watershed, with a small peak at ~40 m. Snow variation in the down-slope direction is also higher than the watershed average at scales of 30 m to 60 m. Because the terrace and riser features lie near the stream feature (100 m to 200 m), topographic variation is also higher in the cross-slope direction at these scales. The peak at 100 to 200 m is completely attenuated in the snow variation, however, demonstrating that at these scales snow redistribution is insensitive to even the largest topographic features in the watershed.

In spite of the complexity present in the watershed, we find that much of the local variation in snow depth can be explained by a very simple model (TM_SV). Developed with the hypothesis that snow depth variation at a given spatial scale is related to topographic variation at the same scale, we model snow depth variation as a weighted sum of the filtered topographic maps, with the weights determined by fitting filtered snow maps at a given scale to filtered topography maps at that same

https://doi.org/10.5194/egusphere-2023-968
Preprint. Discussion started: 22 May 2023

scale . The fitted weights gradually decrease with increasing scale, and topographic information is almost completely attenuated at scales coarser than 100 m (Fig. S3).

Across the watershed, the TM_SV model performs consistently well, with R^2 values greater than 0.5 for 85% of 100 m x 100 m patches, but there are regions where model performance is low. Subpanels d, e, and g of Fig. 4 demonstrate the ability of TM_SV to transform topographic information into a very successful proxy of snow depth at four 100 m x 100 m patches across the watershed. Further, the scale- and directional- dependencies of the simple model are similar to those of snow depth for each topographic feature described previously (Fig. 3). Regions of low TM_SV performance are sites generally located in or near patches of tall shrubs. For example TM_SV model does not work well in the patch presented in subpanels f of Fig. 4, which is characterized by a transition from tundra vegetation to tall shrubs. The success of the simple model across much of the watershed provides strong evidence that snow is redistributed from topographic highs to topographic lows at scales less than 100 m. And, its failure near tall shrub patches suggests that shrub canopies also control snow depth variation in the watershed.

3.2 Snow trapping by shrub canopies

To better understand the influence of shrubs on snow depth variation, we develop an approach that uses machine learning algorithms to quantify shrub canopy snow trapping in complex terrain. The machine learning model performs very well across the watershed, with an R^2 of 0.95 and an RMSE of 9.5 cm, even though only 2% of the data was included in the training set (Fig. S5). The top five most important predictor variables, calculated using the number of times a variable is used for prediction (Elith et al., 2008), include the TM_SV and both shrub potentials, ϕ_1 and ϕ_2 (Table S1). We then set the shrub height and shrub potential to zero everywhere and use the machine learning model to predict snow depth in the absence of shrubs. The difference between the two machine learning models is an estimate of the snow accumulated by shrub canopies throughout the watershed (Fig. 5).

https://doi.org/10.5194/egusphere-2023-968
Preprint. Discussion started: 22 May 2023

Previous work in the watershed predicted that, due to nutrient and water requirements, shrubs grow preferentially in soils covered by thick snowpacks (Shirley et al., 2022). Indeed, many of the shrubs in the watershed are located in regions that have thick snowpacks because of topographic variation (e.g. in the stream bed or next to risers). In these locations, shrub canopies have minimal impact on snow depth. However, there are a number of large patches of tall shrubs across the watershed that are not located in topographic lows. These patches have a strong impact on local snow redistribution, increasing snow depth by more than a meter in some places (Fig. 5). This result suggests that shrub growth and snow accumulation are connected by a positive feedback mechanism.

To better illustrate how snow trapping by shrub canopies varies across the watershed, we focus on the three large shrub patches demarcated in Fig. 6. The impact of each patch on local snow depth is detailed in the subplots of this figure. In all three patches, snow trapping is highest where shrub canopies are densest, but the shrubs also have an impact on snow depth beyond the canopy edges.

Shrub patches, like snow fences, interrupt laminar wind flow, leading to the deposition of suspended snow particles beneath the patches of turbulent air (Pugh and Price, 1954). In Fig. 5, patch A is an isolated patch of shrubs located in a region of relatively uniform topography, which presents an interesting illustration of how shrubs and wind interact to affect snow redistribution. By chance, this patch is shaped like an airfoil positioned at a slight angle to the prevailing wind direction. The pattern of snow trapping near this shrub patch bears a striking resemblance to turbulent airflow paths created by airfoils in historic wind tunnel experiments (Fig. 6). Just as the highest density of turbulent flow is located on the inside edge of the airfoil, most of the snow that is accumulated outside of the shrub canopy is located on the inside edge of the patch. Also, as the turbulent flow extends past the upwind edge of the airfoil, snow is accumulated past the upwind edge of this shrub patch.

Patches B and C, which are located lower in the watershed near stronger topographic features, demonstrate that proximity to other features can change how snow is intercepted near the patch (Fig. 5). In shrub patch B, the impact of canopy trapping on snow depth extends 15-20 m beyond the patch, but rapidly decays. Shrub patch C, however, is ~50 m away from another tall

https://doi.org/10.5194/egusphere-2023-968
Preprint. Discussion started: 22 May 2023

shrub patch. In this patch, the additional snow trapping due to canopy trapping is maintained at 30-50 cm across the entire distance between these two patches. The width of these patches is larger than the distance between them, which is likely important in order to produce this effect. A similar effect can be observed at finer scales within these shrub patches. For example, at meter -20 in panel d, canopy trapping of snow is uninterrupted by a ~20 m gap in the shrub canopy.

3.3 Interannual comparison of snow depth variation

In addition to the 2019 snow maps, we also collected snow depth maps across the watershed at peak snow depth in 2022 (Fig. 1). While there was less snow in 2022 (59 cm on average across the watershed, maximum 439 cm in the stream feature) than in 2019 (100 cm on average, maximum 464 cm in the stream feature), the relationships between topography, vegetation, and snow remained largely consistent between the two years. As in 2019, snow was thickest in topographic lows and in shrub patches in 2022 (Fig. 5, Fig. S4). Further, the relationships between snow variability and spatial scale were largely the same for the stream, terrace, and patterned ground features in both years (Fig. 3).

There are a number of differences in the distribution of snow across the watershed between the two years, however. In particular, there is relatively less snow at the top of the watershed in 2022, and relatively much more snow accumulated in the stream feature in the middle of the watershed (Fig. S6). These differences could be caused by a number of factors. Topography driven snow redistribution could behave differently in low snowpack conditions relative to high snowpack conditions. Or, differences in weather conditions (e.g. high wind speeds, rain-on-snow events, spatial variability in precipitation) between the two years could drive this change. More data is needed to disentangle these potential causes.

We also observe a difference in shrub canopy trapping of snow between the two years. We performed the machine learning analysis of canopy snow trapping using the dataset from 2022, and found increased trapping in 2022 compared to 2019 (Fig. 5, Fig. 7). In many places, snow trapping was ~50 cm greater in the large shrub patches in 2022. We also observe trapping in shorter shrub patches and shrub patches located in topographic lows that did not impact snow depth in 2019. We attribute

https://doi.org/10.5194/egusphere-2023-968
Preprint. Discussion started: 22 May 2023

this difference in shrub canopy snow trapping to lower mean snow depth across the watershed. Since the shrubs rise higher above the snow surface in 2022 than in 2019, more turbulence is created which leads to greater canopy trapping of snow. Indeed, we find that shrub height above the predicted snow surface in the absence of shrubs has a similar relationship to canopy snow trapping in both years (Fig. 7). This trend can be fit with a simple exponential function (R^2 = 0.51, RMSE = 12 cm).

Local (O(~100m)) relationships between topographic variation, vegetation, and snow depth variation are consistent in 2019 (high snowpack) and 2022 (low snowpack), but differences in patterns of snow accumulation at coarser scales between the two years remain unexplained.

4 Conclusions

In this work, we analyze interactions between terrain, vegetation, and snow depth variation using maps of ground, vegetation and snow surface elevation that were collected using an Unmanned Aerial Vehicle (UAV) across a watershed on the Seward Peninsula in Alaska. The novel stacked directional filtering approach presented here is shown to effectively uncover topographic features across scales of interest in complex terrain. We demonstrate that topography controls snow depth variation at scales on the order of 100 m, and show that snow redistribution varies among landscape features. The stacked directional filtering approach could be applied to other research domains in which topography is a strong control, e.g. characterization of the controls on soil moisture across a watershed. This approach offers advantages over traditional topographic indices and streamflow analyses because it extracts information across scales and directions and preserves the shape and sharpness of microtopographic features.

By applying machine learning algorithms to the extracted topographic information and metrics of vegetation distribution, we disentangle the separate impacts of topography and vegetation on snow depth variation across the watershed. We show that canopy trapping in the large shrub patches can increase snow depth by a meter or more. Since shrubs depend on thick

https://doi.org/10.5194/egusphere-2023-968
Preprint. Discussion started: 22 May 2023

snowpacks to warm the soil in this watershed (Shirley et al., 2022), this finding points to the existence of a shrub-snow feedback mechanism that likely plays an important role in the creation of the strong landscape heterogeneity observed in these environments.

To our knowledge, this paper represents the first attempt to quantify snow trapping by natural shrub canopies in morphologically complex landscapes. The simple relationship developed here between shrub structure and snow trapping may be immediately useful for application in high-latitude earth system modeling, particularly since snow trapping by shrub canopies is strongly tied to key processes in these ecosystems (e.g. shrub expansion and permafrost degradation). These findings can also be used to parameterize and test numerical snow-transport models that incorporate both topographic and vegetation information (e.g. SnowModel, (Liston and Sturm, 1998). Future work could leverage these techniques to develop more sophisticated relationships between canopy structure and snow trapping that incorporate information related to shrub density and spatial distribution.

Finally, we compare spatial variation in snow depth across the watershed between two years with very different average snowpacks. While the relationships between topography, vegetation, and snow were similar between years, some differences in the distribution of snow across the landscape were observed. More data and analysis is needed to understand drivers of intra- and inter-annual variability in snow depth distribution across the watershed. Further, similar analyses should be conducted at more watersheds to better understand the impact of variation in aspect, slope, and precipitation on the relationships identified here. This work is needed to develop reliable pan-arctic estimates of snow depth at high spatial resolution.

Acknowledgements

This research was supported by the U.S. Department of Energy, Office of Science, Office of Biological and Environmental Research under Contract No. DE-AC02-05CH11231 to Lawrence Berkeley National Laboratory as part of the Next-Generation Ecosystem Experiments in the Arctic (NGEE-Arctic) project.

https://doi.org/10.5194/egusphere-2023-968
Preprint. Discussion started: 22 May 2023

Data and Code Availability

UAV data and code will be made available at https://ess-dive.lbl.gov/ prior to publication.

References

Avanzi, F., Bianchi, A., Cina, A., De Michele, C., Maschio, P., Pagliari, D., Passoni, D., Pinto, L., Piras, M., and Rossi, L.: Centimetric Accuracy in Snow Depth Using Unmanned Aerial System Photogrammetry and a MultiStation, Remote Sensing, 10, 765, 2018.

Bennett, K. E., Miller, G., Busey, R., Chen, M., Lathrop, E. R., Dann, J. B., Nutt, M., Crumley, R., Dillard, S. L., Dafflon, B., Kumar, J., Robert Bolton, W., Wilson, C. J., Iversen, C. M., and Wullschleger, S. D.: Spatial patterns of snow distribution in the sub-Arctic, https://doi.org/10.5194/tc-16-3269-2022, 2022.

Dafflon, B., Hubbard, S., Ulrich, C., Peterson, J., Wu, Y., Wainwright, H., and Kneafsey, T. J.: Geophysical estimation of shallow permafrost distribution and properties in an ice-wedge polygon-dominated Arctic tundra region, Geophysics, 81, https://doi.org/10.1190/geo2015-0175.1, 2016.

Deems, J. S., Fassnacht, S. R., and Elder, K. J.: Fractal Distribution of Snow Depth from Lidar Data, J. Hydrometeorol., 7, 285–297, 2006.

Dvornikov, Y., Khomutov, A., Mullanurov, D., Ermokhina, K., Gubarkov, A., and Leibman, M.: GIS and field data based modelling of snow water equivalent in shrub tundra, Fennia, 193, 53–65, 2015.

Elith, J., Leathwick, J. R., and Hastie, T.: A working guide to boosted regression trees, J. Anim. Ecol., 77, 802–813, 2008.

Fernandes, R., Prevost, C., Canisius, F., Leblanc, S. G., Maloley, M., Oakes, S., Holman, K., and Knudby, A.: Monitoring snow depth change across a range of landscapes with ephemeral snowpacks using structure from motion applied to lightweight unmanned aerial vehicle videos, The Cryosphere, 12, 3535–3550, 2018.

Frost, G. V., Epstein, H. E., Walker, D. A., Matyshak, G., and Ermokhina, K.: Seasonal and Long-Term Changes to Active-Layer Temperatures after Tall Shrubland Expansion and Succession in Arctic Tundra, https://doi.org/10.1007/s10021-017-0165-5, 2018.

Goetz, J. and Brenning, A.: Quantifying Uncertainties in Snow Depth Mapping From Structure From Motion Photogrammetry in an Alpine Area, Water Resources Research, 55, https://doi.org/10.1029/2019WR025251, 2019.

Greenwell, B., Boehmke, B., Cunningham, J., and Developers, G. B. M.: gbm: Generalized Boosted Regression Models, R package, 2020.

Harder, P., Schirmer, M., Pomeroy, J., and Helgason, W.: Accuracy of snow depth estimation in mountain and prairie environments by an unmanned aerial vehicle, The Cryosphere, 10, 2559–2571, 2016.

Harder, P., Pomeroy, J. W., and Helgason, W. D.: Improving sub-canopy snow depth mapping with unmanned aerial vehicles: lidar versus structure-from-motion techniques, The Cryosphere, 14, 1919–1935, 2020.

James, M. R. and Robson, S.: Straightforward reconstruction of 3D surfaces and topography with a camera: Accuracy and geoscience application, Journal of Geophysical Research: Earth Surface, 117, 2012.

Konduri, V., Breen, A., Hargrove, W., Hoffman, F., Salmon, V., Iversen, C., Ganguly, A., and Kumar, J.: Hyperspectral remote sensing-based plant community map for region around NGEE-Arctic intensive research watersheds at Seward Peninsula, Alaska, 2017-2019, https://doi.org/ 10.5440/1828604, 2022.

Léger, E., Dafflon, B., Robert, Y., Ulrich, C., Peterson, J. E., Biraud, S. C., Romanovsky, V. E., and Hubbard, S. S.: A distributed temperature profiling method for assessing spatial variability in ground temperatures in a discontinuous permafrost region of Alaska, https://doi.org/10.5194/tc-13-2853-2019, 2019.

Liston, G. E. and Sturm, M.: A snow-transport model for complex terrain, https://doi.org/10.1017/s0022143000002021, 1998.

https://doi.org/10.5194/egusphere-2023-968
Preprint. Discussion started: 22 May 2023

Meloche, J., Langlois, A., Rutter, N., McLennan, D., Royer, A., Billecocq, P., and Ponomarenko, S.: High-resolution snow depth prediction using Random Forest algorithm with topographic parameters: A case study in the Greiner watershed, Nunavut, Hydrological Processes, 36, https://doi.org/10.1002/hyp.14546, 2022.

Myers-Smith, I. H. and Hik, D. S.: Shrub canopies influence soil temperatures but not nutrient dynamics: An experimental test of tundra snow-shrub interactions, https://doi.org/10.1002/ece3.710, 2013.

Nolan, M., Larsen, C., and Sturm, M.: Mapping snow depth from manned aircraft on landscape scales at centimeter resolution using structure-from-motion photogrammetry, The Cryosphere, 9, 1445–1463, 2015.

O'Neill, H. B. and Burn, C. R.: Talik Formation at a Snow Fence in Continuous Permafrost, Western Arctic Canada, https://doi.org/10.1002/ppp.1905, 2017.

Pugh, H. L. D. and Price, W. I. J.: Snow drifting and the use of snow fences, https://doi.org/10.1017/s0032247400042753, 1954.

Reu, J. D., De Reu, J., Bourgeois, J., Bats, M., Zwertvaegher, A., Gelorini, V., De Smedt, P., Chu, W., Antrop, M., De Maeyer, P., Finke, P., Van Meirvenne, M., Verniers, J., and Crombé, P.: Application of the topographic position index to heterogeneous landscapes, https://doi.org/10.1016/j.geomorph.2012.12.015, 2013.

Revuelto, J., Billecocq, P., Tuzet, F., Cluzet, B., Lamare, M., Larue, F., and Dumont, M.: Random forests as a tool to understand the snow depth distribution and its evolution in mountain areas, Hydrol. Process., 34, 5384–5401, 2020.

Revuelto, J., Alonso-Gonzalez, E., Vidaller-Gayan, I., Lacroix, E., Izagirre, E., Rodríguez-López, G., and Ignacio López-Moreno, J.: Intercomparison of UAV platforms for mapping snow depth distribution in complex alpine terrain, Cold Reg. Sci. Technol., 190, 103344, 2021.

Shirley, I. A., Mekonnen, Z. A., Wainwright, H., Romanovsky, V. E., Grant, R. F., Hubbard, S. S., Riley, W. J., and Dafflon, B.: Near-Surface Hydrology and Soil Properties Drive Heterogeneity in Permafrost Distribution, Vegetation Dynamics, and Carbon Cycling in a Sub-Arctic Watershed, https://doi.org/10.1029/2022jg006864, 2022.

Shirley, I. A., Mekonnen, Z. A., Grant, R. F., Dafflon, B., and Riley, W. J.: Machine learning models inaccurately predict current and future high-latitude C balances, Environ. Res. Lett., 18, 014026, 2023.

Smith, M. W. and Riseborough, D. W.: Climate and the limits of permafrost: a zonal analysis, https://doi.org/10.1002/ppp.410, 2002.

Sturm, M., Schimel, J., Michaelson, G., Welker, J. M., Oberbauer, S. F., Liston, G. E., Fahnestock, J., and Romanovsky, V. E.: Winter Biological Processes Could Help Convert Arctic Tundra to Shrubland, https://doi.org/10.1641/0006-3568(2005)055[0017:wbpchc]2.0.co;2, 2005.

Uhlemann, S., Dafflon, B., Peterson, J., Ulrich, C., Shirley, I., Michail, S., and Hubbard, S. S.: Geophysical Monitoring Shows that Spatial Heterogeneity in Thermohydrological Dynamics Reshapes a Transitional Permafrost System, https://doi.org/10.1029/2020gl091149, 2021.

Wainwright, H. M., Liljedahl, A. K., Dafflon, B., Ulrich, C., Peterson, J. E., Gusmeroli, A., and Hubbard, S. S.: Mapping snow depth within a tundra ecosystem using multiscale observations and Bayesian methods, https://doi.org/10.5194/tc-11-857-2017, 2017.

Wipf, S. and Rixen, C.: A review of snow manipulation experiments in Arctic and alpine tundra ecosystems, https://doi.org/10.1111/j.1751-8369.2010.00153.x, 2010.

Zhang, T.: Influence of the seasonal snow cover on the ground thermal regime: An overview, https://doi.org/10.1029/2004rg000157, 2005.

Zoltai, S. C.: Cyclic Development of Permafrost in the Peatlands of Northwestern Alberta, Canada, https://doi.org/10.2307/1551820, 1993.

https://doi.org/10.5194/egusphere-2023-968
Preprint. Discussion started: 22 May 2023

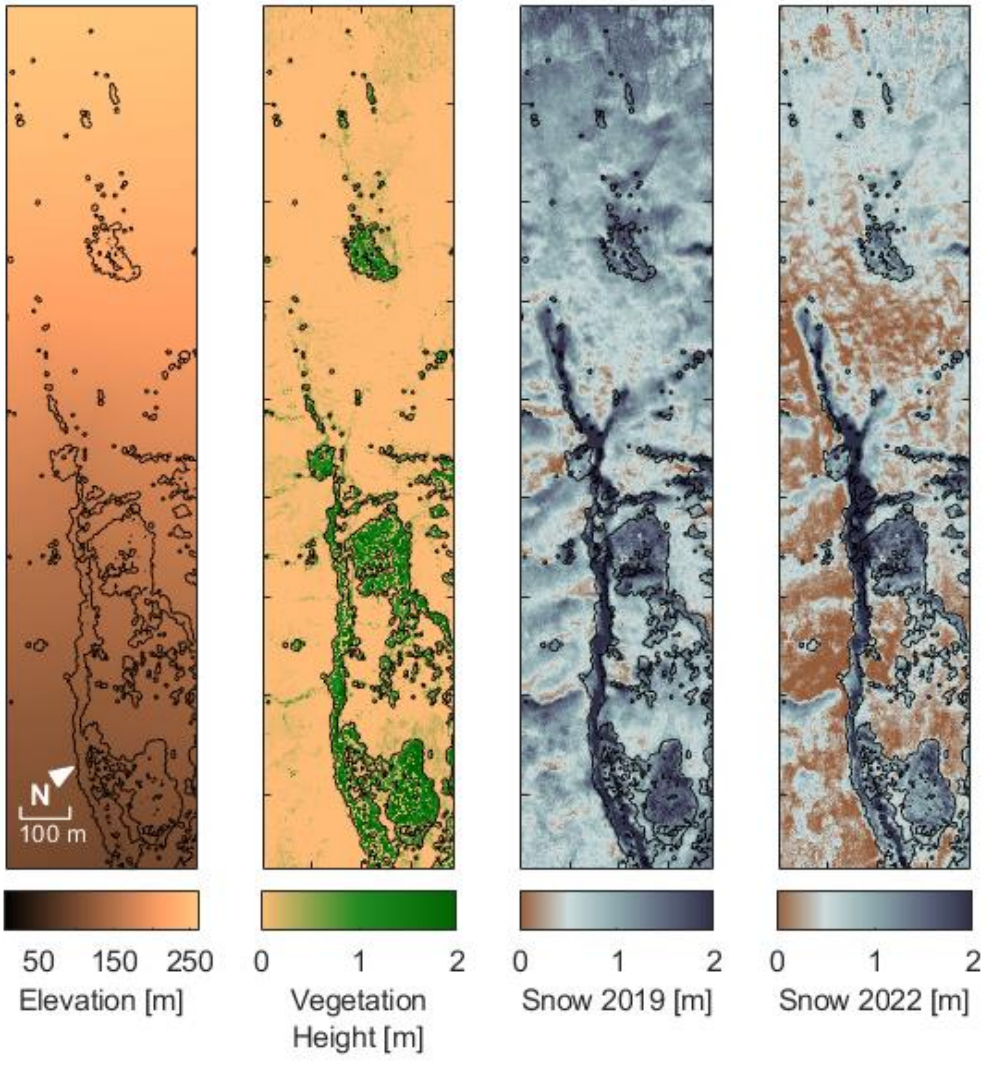

415

Figure 1. Digital terrain map, vegetation height, and snow depth. Digital terrain map (DTM), vegetation height, and snow depth in 2019 and 2022 are shown for the studied watershed. Snow depths in the stream feature can be as high as 4.5 m in both 2019 and 2022, but we limit the ranges of these figures to show snow depths up to 2 m for clarity. Contour lines are drawn at a 3 m distance from vegetation of 1 m height or taller.

420

https://doi.org/10.5194/egusphere-2023-968
Preprint. Discussion started: 22 May 2023

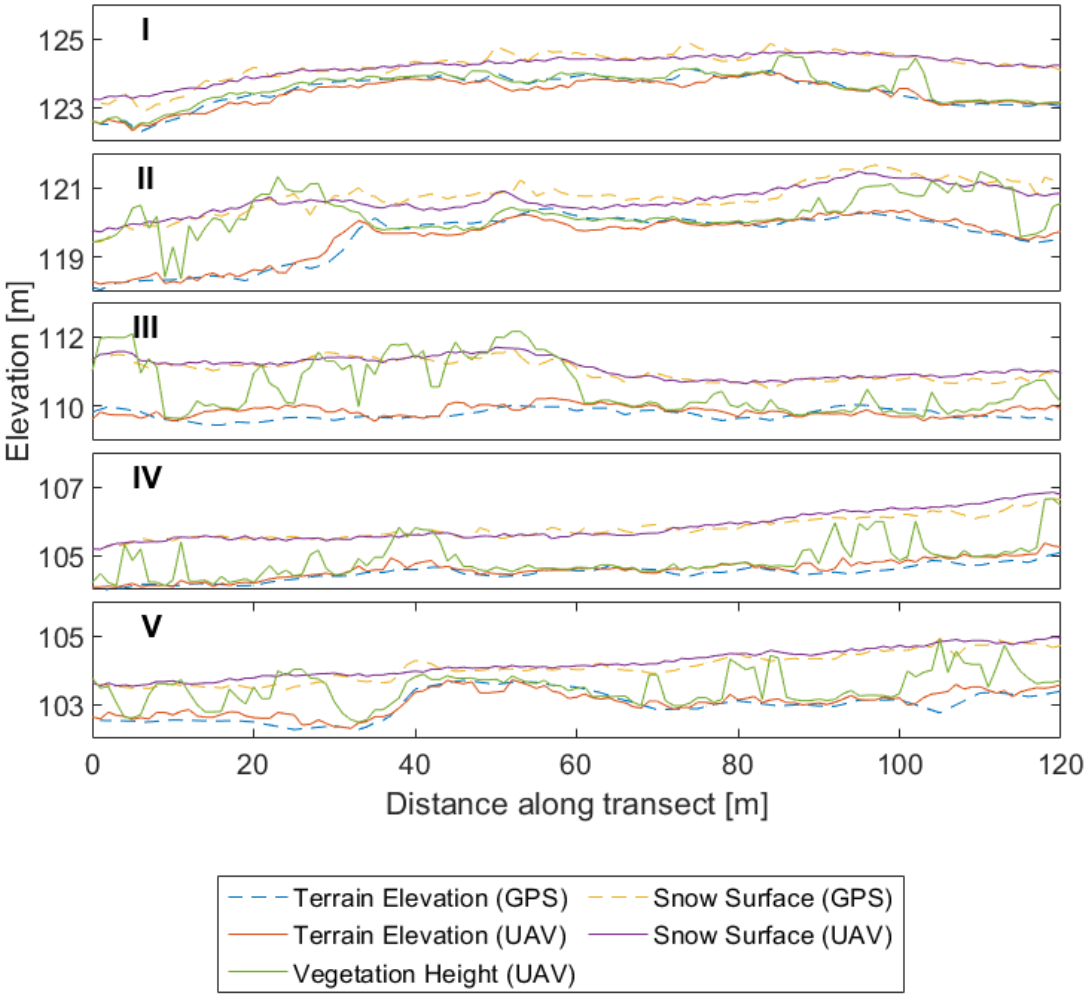

Figure 2. Validation of digital terrain map and snow depth. UAV-derived snow depth products were validated using transects of RTK-GPS measurements. Orthomosaic of the transects and surrounding area is shown on the left. Contour lines are drawn at a 3 m distance from vegetation of 1 m height or taller. A snow depth map of the transects and surrounding area is shown in the middle. Contour lines are drawn at terrain elevation isolines with a spacing of 1m. UAV and RTK-GPS measurements for each transect are shown on the right. The terrain surface measured by RTK-GPS (blue, dashed) and extracted from UAV imagery (red), the snow surface measured by RTK-GPS (orange, dashed) and extracted from UAV imagery (purple), and the vegetation height extracted from UAV imagery (green) are shown for each transect.

https://doi.org/10.5194/egusphere-2023-968
Preprint. Discussion started: 22 May 2023

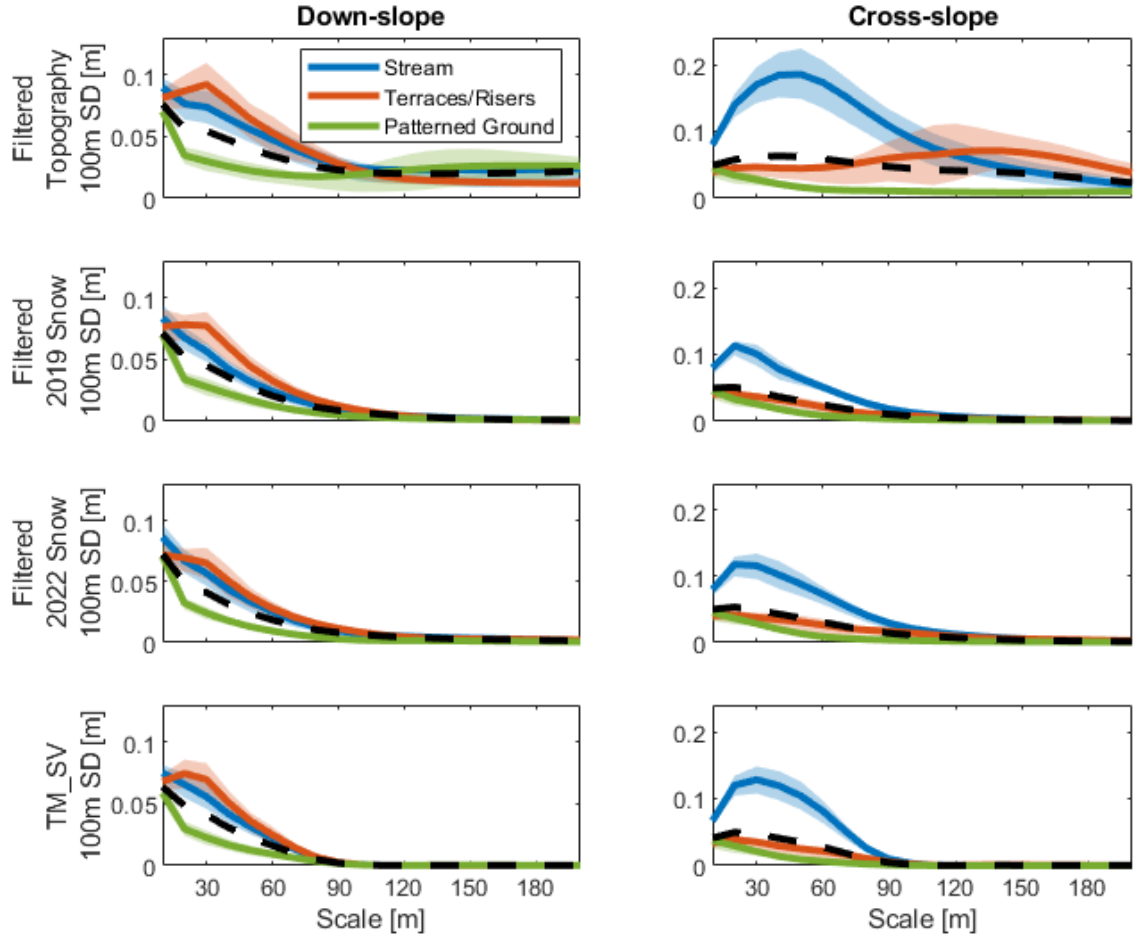

Figure 3. Scale- and directional-dependence of topography, snow, and topographic model of snow depth variation (TM_SV) for each feature. Standard deviation (SD) of 100 m x 100 m patches at each scale is shown for the filtered topographic maps (top row), filtered snow depth maps in 2019 (second row) and 2022 (third row), and the TM_SV model (bottom row) in both the down-slope (left column) and cross-slope (right column) directions. In each panel, the mean (solid lines) and 25th-75th percentile ranges (shaded regions) for the 100 m x 100 m patches are shown for the stream feature (blue), terrace and riser features (red), and the patterned ground (green). The watershed mean is shown as a black, dashed line.

https://doi.org/10.5194/egusphere-2023-968
Preprint. Discussion started: 22 May 2023

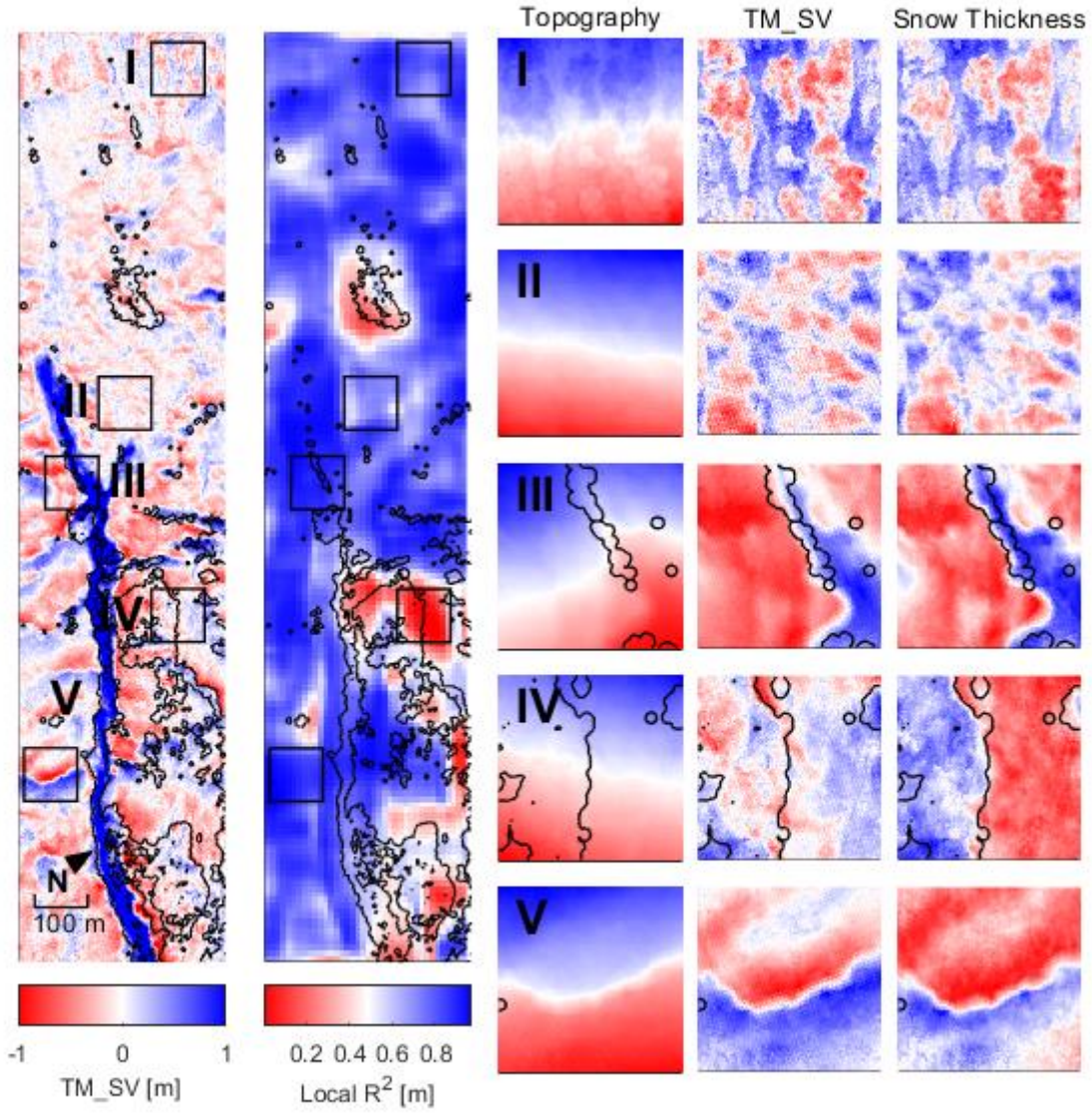

Figure 4. Topographic model of snow depth variation (TM_SV). The topographic model of snow depth variation (TM_SV) across the watershed is shown on the left. R^2 values for linear fits of 100 m x 100 m subsets of the TM_SV to 100 m x 100 m subsets of 2019 snow depth are shown in the middle. Maps of mean-centered topography, TM_SV, and 2019 snow depth are shown for five example 100 m x 100 m subsets on the right. Contour lines are drawn at a 3 m distance from vegetation of 1 m height or taller.

https://doi.org/10.5194/egusphere-2023-968
Preprint. Discussion started: 22 May 2023

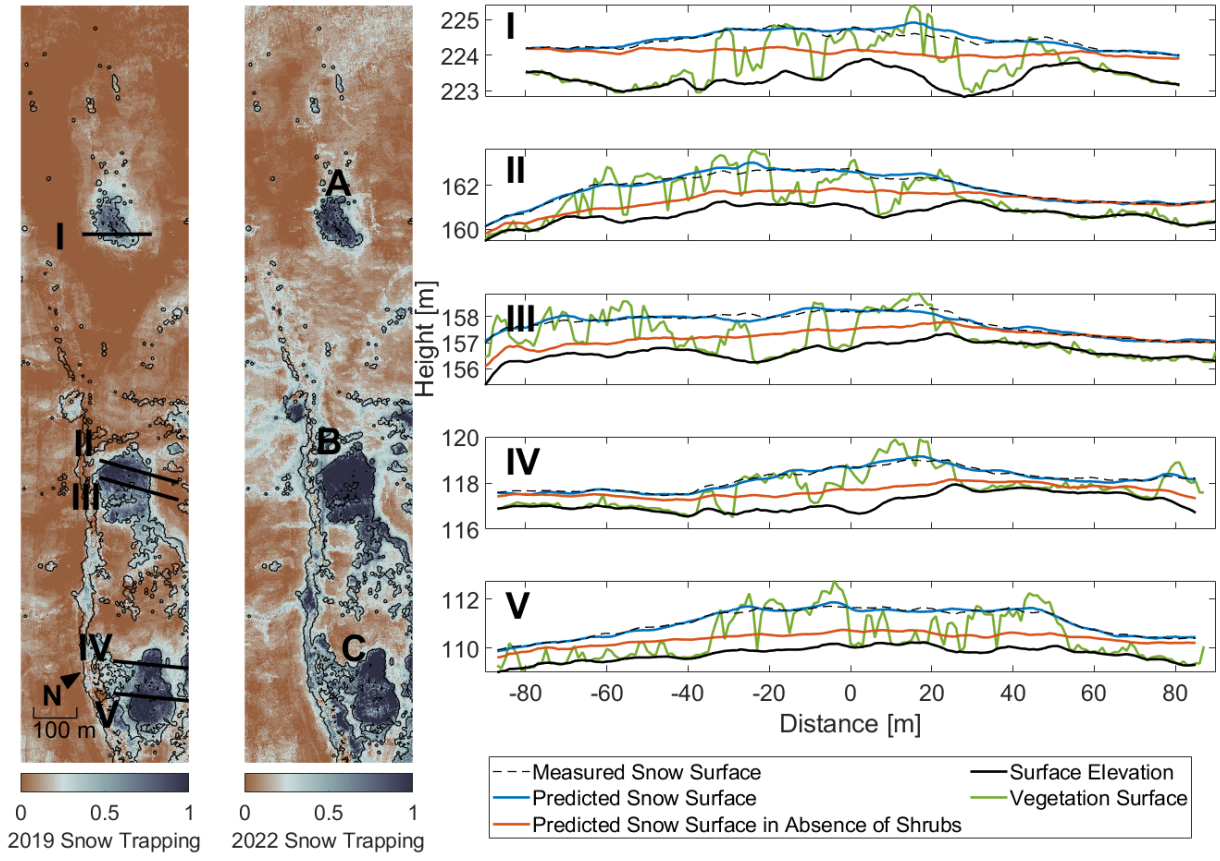

Figure 5. Snow trapping by shrub canopies. Modeled snow trapping by shrubs across the watershed is shown for 2019 (left) and 2022 (middle). Contour lines are drawn at a 3 m distance from vegetation of 1 m height or taller, large shrub patches A, B, and C are labeled in the middle panel, and the locations of five transects that cross the large shrub patches are shown in the left panel. The measured snow surface (black, dashed), predicted 2019 snow surface (blue), predicted 2019 snow surface in the absence of shrubs (red), terrain elevation (black), and vegetation surface (green) are shown for each transect on the right.

https://doi.org/10.5194/egusphere-2023-968
Preprint. Discussion started: 22 May 2023

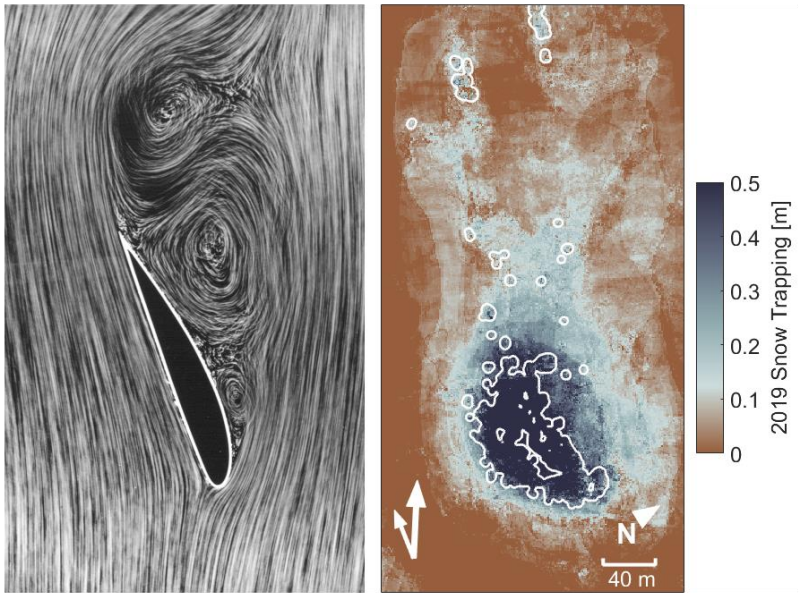

Figure 6. Turbulent airflow and snow trapping by shrub canopies. Turbulent airflow created by an airfoil in an historic wind tunnel experiment is shown on the left (*Photo: DLR, CC-BY 3.0*). 2019 snow trapping by shrub patch A is shown on the right. White arrows denote the prevailing wind direction in the watershed between December 2018 and March 2019 for wind speeds greater than 5 m/s (small arrow) and wind speeds greater than 10 m/s (large arrow). Wind speeds and directions are taken from a weather station at the top of the watershed (Busey et al. 2017). Contour lines are drawn at a 3 m distance from vegetation of 1 m height or taller.

https://doi.org/10.5194/egusphere-2023-968
Preprint. Discussion started: 22 May 2023

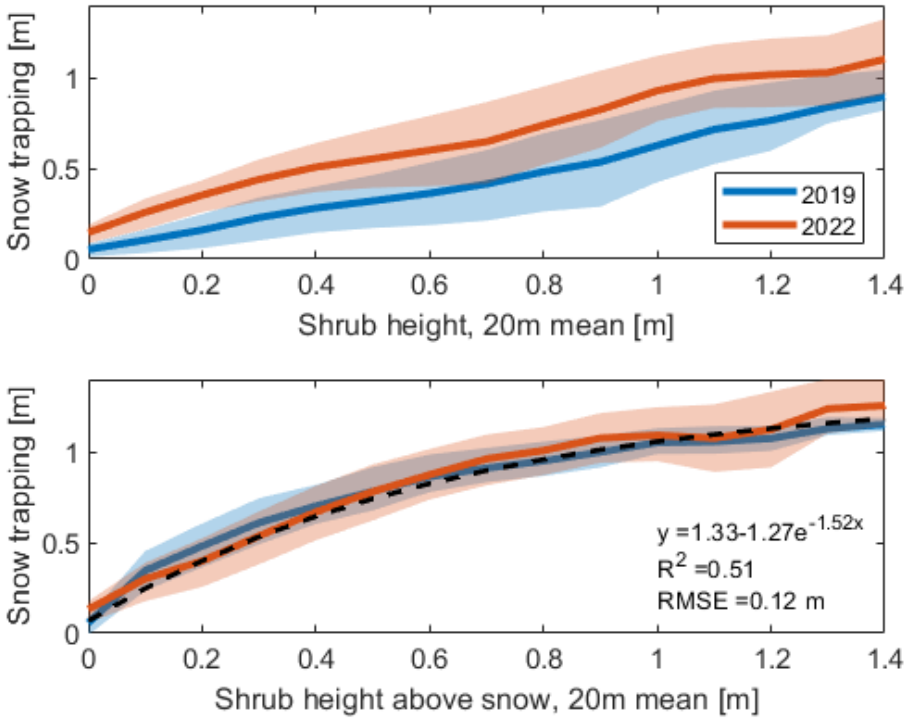

Figure 7. Snow trapping as a function of shrub canopy height. Mean (solid lines) and 25th-75th percentile (shaded regions) snow trapping by shrub canopies for 2019 (blue) and 2022 (red) is plotted as a function of 20 m mean shrub height (top) and as a function of 20 m mean shrub height above the modeled snow surface in the absence of shrubs (bottom). An exponential curve fit to the 2019 and 2022 data is shown in the bottom panel (black, dashed).